Identification and Extraction of Surface Waves from Three-Component Seismograms Based on the Normalized Inner Product — Source link

Kristel C. Meza-Fajardo, Apostolos Papageorgiou, Jean-François Semblat

Institutions: Universidad Nacional Autónoma de Honduras, University of Patras, IFSTTAR

Published on: 01 Feb 2015 - Bulletin of the Seismological Society of America (Seismological Society of America)

Topics: Love wave, Rayleigh wave, Time–frequency analysis, Wave propagation and Surface wave

Identification and Extraction of Surface Waves from Three-component Seismograms based on the Normalized Inner Product

Kristel Carolina Meza Fajardo, Apostolos Papageorgiou, Jean-François Semblat

TITLE:

Identification and Extraction of Surface Waves from Three-component Seismograms based on the Normalized Inner Product

AUTHORS' NAMES:

Kristel C. Meza-Fajardo[(1)], Apostolos S. Papageorgiou[(2)] and Jean-François Semblat[(3)]

CORRESPONDING AUTHOR:

Kristel C. Meza-Fajardo

Department of Civil Engineering,

Universidad Nacional Autónoma de Honduras

Tegucigalpa, Honduras

E-mail: kristelmeza@unah.edu.hn

ABSTRACT

Identification of different wave types in a seismogram is an important step for the understanding of wave propagation phenomena. Since in most seismograms, different types of waves with different frequencies may appear simultaneously, separation of waves is more effectively achieved when a time-frequency analysis is performed. In this work, we propose a new time-frequency analysis procedure to identify and extract Rayleigh and Love waves from three-component seismograms. Exploiting the advantage of the absolute phase preservation by the Stockwell Transform, we construct time-frequency filters to extract waves based on the 'Normalized Inner Product' (NIP). Since the NIP is the time-frequency counterpart of the correlation, Rayleigh and Love waves can be identified depending on the NIP between the Stockwell Transforms of the horizontal and vertical displacement components. The novelty and advantage of the proposed procedure is that it does not require specifying a-priori the direction of propagation of the surface waves, but instead such direction is determined. Furthermore, it is shown that the NIP is a more stable parameter in the time-frequency domain when compared to the instantaneous reciprocal ellipticity, and thus it avoids smoothing (and with it, altering) the data. The procedure has been successfully tested with real signals, specifically to extract Rayleigh and Love waves from seismograms of one aftershock of the 1999 Chi-Chi earthquake. With the proposed procedure we found different directions of propagation for retro-grade and pro-grade Rayleigh waves, which might suggest that they are generated by different mechanisms.

INTRODUCTION

The identification of surface waves in a time history is one of the fundamental tasks in seismology. Surface waves are important not only because they carry information about the surficial geological layers in which they propagate, but also for their impact on man-made structures. Methods for identifying surface waves are based on the two main characteristics of such waves: (1) plane and type of polarization, and (2) frequency-dependent phase velocities (dispersion). A processor to identify surface waves and simultaneously compute their azimuth, was proposed in the late 70's by Smart (1978). The algorithm finds the best fit between polarization characteristics of ground motion and surface wave models defined in the frequency domain. More recently, identification of Rayleigh wave phases has been performed by means of Complex Trace Analysis (CTA) (Vidale, 1986, René *et al*., 1986, Li and Crampin, 1991, Baker and Stevens, 2004). CTA uses time-varying polarization characteristics to differentiate between waves, and thus, waves arriving at different times can be separated. Rayleigh waves are identified by considering the fact that they are elliptically polarized in a plane oriented in their direction of propagation. However, in view of the fact that dispersed waves (such as surface waves) may be effectively described and analyzed in terms of narrow-band wave packets, we need an extraction technique that resolves the recorded signals in such narrow-band packets. Since CTA does not provide information on the time variation of the frequency content of the signal, the analyst needs to choose frequency ranges of interest *a priori*. This problem is aggravated when different types of waves appear simultaneously in the signal under investigation, as it often happens with seismic waves. Another difficulty faced by the analyst is the need to assume *a priori* the direction of propagation of the surface waves present in the time histories.

Considering the above reasons, a time-frequency polarization analysis seems to be a more appropriate alternative in order to separate the different phases in a wave field. Whereas most of classical signal processing studies of the 1970s were aimed at stationary signals and processes, many efforts were devoted to less idealized situations during the 1980s, and the idea of time-frequency analysis progressively emerged as a new paradigm for non-stationarity. It is now well recognized that many signal processing problems can be advantageously phrased in a time-frequency language. Pinnegar (2006) and Galiana-Merino *et al*. (2011) have constructed filters to exclude or extract Rayleigh waves using their elliptical polarization as filtering criterion. However, filtering based on the elliptical polarization attribute alone does not work well if the time history contains Rayleigh waves with both retro-grade and pro-grade motion. Such a case has been observed in recordings of the aftershock 1803 of the Chi-Chi earthquake that occurred on 20 September 1999 with magnitude Mw 6.2 (Wang *et al*., 2006). The method we propose herein to detect and extract surface waves from three-component recorded seismograms overcomes these difficulties. We exploit the advantage of the absolute phase preservation of the Stockwell Transform (Stockwell *et al*., 1996), and we construct time-frequency filters to extract waves based on the 'Normalized Inner Product' (NIP). Since the NIP is the time-frequency counterpart of the correlation, Rayleigh and Love waves can be identified based on the value of the NIP between the Stockwell Transforms of the horizontal and vertical displacement components. The proposed procedure does not require specifying a-priori the direction of propagation of the surface waves, but instead such direction is determined with the proposed computational procedure.

TIME-FREQUENCY POLARIZATION ANALYSIS

Polarization characteristics are useful tools to identify and separate different types of waves present in a multi-component signal. If the components of the analyzed signal are in-phase, it is said that they are linearly polarized. When the components are 90 degrees out-of-phase and have the same amplitude, the state corresponds to circular polarization. If the components are 90 degrees out-of-phase and have different amplitudes, the state corresponds to elliptical polarization. Regarding waves contained in seismic signals, the polarization state observed for Rayleigh waves is elliptical (either retro-grade or pro-grade), whereas body and Love waves are considered to be linearly polarized.

Following the ideas presented by Pinnegar (2006), three-component signals can be thought as a superposition of sinusoids oscillating along the -, -, and - axes, which when considered one frequency at a time, trace out elliptical motion in 3D space. Thus, the total three component signal can be thought of as a superposition of ellipses, which are characterized by descriptive parameters such as the length of the semi-minor and semi-major axis, the strike and dip of each ellipse plane, the pitch of the major axis, and the phase of the particle motion at each frequency. The Fourier spectra of the descriptive parameters of the superimposed ellipses can be related to the Fourier transforms of the -, - and - components (Pinnegar, 2006). The same type of reasoning can be used with windowed Fourier transforms (such as the Stockwell Transform), so as to provide time-varying spectra for the abovementioned descriptive parameters. Details on how the attributes of the ellipses are defined for three-component signals can be found in Pinnegar (2006).

In this work, we adopt the Stockwell Transform for the mapping between time and time-frequency domains, because: 1) using the Stockwell Transform, we retain the absolute phase of each localized frequency component (Stockwell *et al*., 1996), and 2) the invertibility of the Stockwell Transform allows for the wave extraction by simple filtering in the time-frequency domain. The Stockwell Transform is a generalization of the short-time Fourier transform (STFT), and may be thought of as an extension of the continuous wavelet transform (CWT) while overcoming some of its disadvantages. It is based on a moving and scalable localizing Gaussian window, which features a standard deviation that is always equal to one wavelength of the Fourier sinusoid (Pinnegar, 2006). The "moving window" technique has been already used in the past in surface wave analyses (Flinn, 1965; Dziewonski *et al*., 1969; Vidale, 1986) based on the concept of the "analytical signal" of the time series. It can be shown (Stockwell, 2007) that the Stockwell Transform at a specific frequency is closely related to the analytical signal of the time series, when the time series is bandpass filtered using the Gaussian window. The Stockwell transform of a time varying function can be expressed in the following form (Stockwell *et al*., 1996):

(1)

where is the center of the Gaussian window. The time-frequency parameters of the polarization ellipse, which describe the contribution of the -th frequency to the total signal are defined in Pinnegar (2006) in terms of the Stockwell transform. In particular, Pinnegar (2006) and Galiana-Merino *et al*. (2011) have used the ratio of the semi-minor to the semi-major axis of the polarization ellipse to identify Rayleigh waves contained in a seismic signal. This ratio is called in Galiana-Merino *et al*. (2011) "instantaneous reciprocal ellipticity" (IRE), and is defined as:

(2)

where and are the semi-major and semi-minor axis of the ellipse, respectively. For a three-component signal these axes are given by the following expressions (Pinnegar 2006):

(3)

where

(4)

Here and are the real and imaginary parts of the Stockwell transform of the -component of the signal (we omit the arguments to avoid clutter). Similarly, ( ) and ( ) are pairs of the real and imaginary parts of the Stockwell transform for the - and - components of the signal, respectively. Note that the major axis of the polarization ellipse is composed of two parts, and . Since the semi-minor axis corresponds to the radius of the circular polarization, the segment will be the part corresponding to linear polarization. Therefore, if the polarization state is circular, , and consequently If the polarization is linear, and then The IRE can then be used to discern the different waves contained in a seismic signal. To identify Rayleigh waves, Galiana-Merino *et al*. (2011) and Pinnegar (2006) have considered values of greater than . Using this criterion, filters to extract the desired wave from the signal can be readily constructed. The filters are applied in the time-frequency domain , and then the Inverse Stockwell Transform is used to recover the filtered time-domain signal. The Inverse Stockwell Transform is computed in two steps:

first, the Fourier Transform of the original signal is obtained by integrating the Stockwell transform over time , and then the Fourier Transform is inverted (Stockwell *et al*., 1996).

Galiana-Merino *et al*. (2011) made use of the IRE to extract Rayleigh waves adopting the Stationary Wavelet Packet Domain (SWPD) method. However their approach requires knowledge, in advance, of the direction of propagation of the Rayleigh waves in order to be applied. In Galiana-Merino *et al*. (2011) it is suggested that this direction will be the "radial" direction of wave propagation (i.e. the back-azimuth to the epicenter). However this assumption may not be correct if the waves are generated by diffraction at the edge of a basin, or if they are waves trapped inside the basin. Thus, in Galiana-Merino *et al*. (2011) the horizontal components are rotated to obtain the radial component and then, the vertical and radial components are used to compute the IRE. On the contrary, the IRE, defined by Pinnegar (2006) as in Eq. (2), is computed using the three components of the signal and it does not change when the horizontal components are rotated. However, even after extracting the waves (i.e. their components along two arbitrary orthogonal axes), their direction of propagation is not provided by the filtering process using the value of the IRE as the criterion.

DIRECTION OF SURFACE WAVE POLARIZATION

Once the polarization filtering has been completed, the angle of propagation of the extracted Rayleigh waves may be estimated by correlating the filtered signals. One way to accomplish this is to use the Chael-Selby-Baker-Stevens technique of calculating the back-azimuth of Rayleigh waves (Chael, 1997; Selby, 2001; Baker and Stevens, 2004). The basic idea of this approach is to find an azimuth for which the vertical and Hilbert-transformed radial component particle motions form a straight line (i.e. they are linearly polarized). First, the two horizontal components are rotated into assumed radial and transverse directions, with a trial back-azimuth ranging from to . The computed radial component is then shifted in time using the Hilbert Transform. The shift must be a phase delay for pro-grade motion or phase advance for retro-grade motion (see Figure 1). The last step is the computation of the cross correlation between the vertical and Hilbert-transformed horizontal (radial) traces with the following formula:

(5)

where

, , or (6)

the function is the vertical displacement component and is the Hilbert-transformed radial displacement component. The estimated direction of the Rayleigh wave propagation corresponds to the direction ( ) that provides the maximum correlation, as sweeps the range to .

Clearly, the Chael-Selby-Baker-Stevens technique is a procedure that relies on sweeping the entire parameter space and selecting the value that returns the highest correlation. Here we propose a more direct procedure to compute the direction of propagation of the surface waves. Let us assume that the recorded motion consists of three components: along the N-S direction (positive pointing to the North); along E-W direction (positive pointing to the East); and in the vertical direction (positive pointing up). Then, if the above-defined horizontal components were rotated by an angle (positive clockwise, as shown in Figure 2), so as to render: the radial component (along the direction of propagation; positive direction pointing away from the source/origin of the dispersive wave); and the transverse component (in the transverse direction, obtained by rotating the radial direction clockwise by (π/2), as shown in Figure 2). To derive an expression to directly compute , we start by relating the horizontal components and to the components and as follows:

(7)

If the radial component and the shifted (Hilbert Transformed) vertical component are in phase, then we can reasonably consider that these are the components of a Rayleigh wave, which, in turn, implies that, the correlation coefficient of the transverse component and should ideally be zero (in essence we are assuming that the identified Rayleigh wave is not correlated with the linearly polarized wave in the transverse direction, if such a wave exists). Under this assumption, Eq. (5) leads to:

(8)

Substitution of the second equation given in (7) in the above expression leads to:

(9)

Solving this equation for we obtain the average direction of propagation of the wave train:

(10)

where the subscript is added because Eq. (10) provides only the 'reference' angle of the direction of propagation of the Rayleigh waves. The azimuth in its correct quadrant can be computed with the expressions:

(11)

which can be condensed in the following single equation:

(12)

where is the sign function. Note that Eqs. (11) and (12) take into account the sign of reference angle , which will have the same sign as . If the extracted signal is composed of more than one dispersive wave propagating in distinct, albeit similar, directions, then, Eq. (10)-(12) should be applied independently to each one of them. By inspecting the Stockwell Transform of the signal the analyst can observe if there are several wave trains.

The time-domain procedures to compute the direction of propagation of Rayleigh waves presented in this section work well if the waves have already been identified and extracted. An implicit assumption in those procedures is that Rayleigh waves are either pro-grade or retro-grade, but not a mixture. Retro-grade particle motion is usually the type of polarization expected for Rayleigh waves. However, some geological settings allow for the generation of both retro-grade and pro-grade waves. One example is the West Coastal Plain in Taiwan, as reported by Wang *et al.* (2006). With the IRE criterion as defined in Eq. (2) it is not possible to identify whether the particle motion is pro-grade or retro-grade. Galiana-Merino *et al*. (2011) suggest the instantaneous phase difference between the Radial and Vertical components can be used to discern between these two types of motion. However, this requires knowledge of the angle specifying the radial direction, and in most cases this angle is not available to the analyst. This is why we propose a new criterion to filter the components of the signal to extract Rayleigh waves, which does not require the specification of their direction of propagation, and differentiates between pro-grade and retro-grade motion. This criterion is the Normalized Inner Product (NIP) that we define in the following section.

THE NORMALIZED INNER PRODUCT

Let the Stockwell Transforms of the North, East and Vertical components of the signal be denoted by , , , respectively. In a similar manner, we denote the Stockwell Transforms of the radial and transverse component of the signal by and . We recognize that each of the discrete Stockwell Transforms is a matrix defined in the discretized space. Furthermore, each element , of the discretized space is a complex number and may be expressed as follows:

(13)

We find it convenient to treat each element as a two-element vector; *e.g.* for the vertical component , we define:

(14)

with corresponding definitions for the radial, transverse, North and East components, , , , , respectively. Once we treat each element of the discretized space as a vector, we can define inner (dot) products with them. For example, the inner product of the radial with the vertical component can be expressed as:

(15)

The inner product allows one to take advantage of the following facts: 1) the phase of the Stockwell Transform is absolutely referenced, (2) when normalized, the inner product is (in a way) the time-frequency counterpart of the correlation in the time domain. Therefore, for a Rayleigh wave, if we shift appropriately (i.e. by a phase-delay for pro-grade particle motion, or by phase-advance for retro-grade particle motion) the vertical component, then the shifted vertical component should be in-phase with the radial component. If we refer to the shifted vertical component by , then ideally , and . Practically, we expect the difference] to be small and, consequently, we expect to attain values close to 1. Making use of the definitions established earlier, the Normalized Inner Product of the radial and appropriately shifted vertical components, denoted by is given by:

(16)

Note that in the time-frequency domain, the time shifted vertical component is obtained simply by multiplying the positive frequencies of by − for a phase advance, and by − for a phase delay. Then, we can construct simple filters to retain only those regions in the space where the value of the is close to 1 (say,) and setting the rest of the space equal to zero. Following Pinnegar (2006), the filters can be alternatively defined using continuous functions by means of cosine tapers, to reduce numerical artifacts when the filtered transforms are inverted to recover the extracted waves.

Since we do not know the direction of propagation of the Rayleigh wave, the elements cannot be computed directly applying the Stockwell Transform to some time history in such direction. Here we propose an indirect method to compute the elements . Exploiting the linearity of the Stockwell Transform, we obtain the time-frequency counterpart of Eq. (7):

(17)

In order to find the azimuth , we again make use of the fact that, for a Rayleigh wave, the correlation between the transverse component and the shifted vertical component is zero:

(18)

Following a similar reasoning to the one presented in the previous section, the time-frequency counterpart of Eq. (10) can be expressed as:

$$— \quad - \quad - \qquad (19)$$

Here is a function of , and is expected to present small variations when associated to a wave train. If several wave trains are present in the signal, having different directions of propagation, Eq. (19) is valid for each of the corresponding time intervals. Now, taking in consideration the quadrants in the N-S, E-W plane, the azimuth giving the direction of propagation of the wave train is given by:

$$- \qquad (20)$$

where

(21)

and if the sense of propagation of the wave train is towards the East, whereas if the sense of propagation of the wave train is towards the West. The determination of the sense of propagation can be accomplished if the position of the source/origin of the signal is known, or if we have more than one station recording the propagating dispersive wave. Let us emphatically note that if the sense of propagation, of the phase under investigation, is not established, pro-grade or retro-grade motion cannot be defined without ambiguity. Also, let us note that sense of propagation and direction of propagation are not the same thing. The direction is given by a numerical value of , whereas the sense of propagation only indicates whether the propagation of the wave train is towards the East or the West. Once the angle is computed, the elements can be computed in the time-frequency domain with the first equation given in (17).

The NIP criterion is particularly useful when in the seismogram we have simultaneously the traces of pro-grade and retro-grade Rayleigh waves. These waves may be associated with different frequencies if the physical processes that generate them are different. Since the NIP criterion we use is defined in terms of , the filter constructed with this criterion will exclude the regions of the space that are associated with pro-grade particle motion if has been obtained with a phase advance. Conversely, the filter will exclude the regions of the space corresponding to retro-grade motion if has been obtained with a phase delay (Figure 1).

After the filters are applied to the time-frequency components of the signal, the filtered Stockwell Transforms are inverted and what we eventually obtain are Rayleigh waves with only pro-grade or retro-grade particle motion (depending on how we shifted the vertical component). The radial, transverse and vertical components can then be obtained by either of the following two approaches:

1) Applying the filter to the , and components, and inverting the resulting Transforms to obtain the North-East-Vertical components of the extracted wave train. Then, the radial-transverse components are obtained by rotation of the North-East components with the azimuth calculated with Eq. (12).

2) The filter is applied to the , and components. Let us recall that the and components are computed with Eq. (17). The time-domain radial and transverse components of the wave train are obtained directly by inverting the filtered Transforms.

Extraction of Love Waves

The criterion is also useful for the extraction of Love waves, which are dispersive waves linearly polarized on the horizontal plane along a direction which is transverse to the direction of propagation. In the case of a noise-free synthetic signal which consists of only linearly polarized waves on the horizontal plane, would be zero and apparently Eq. (19) could not be used. However if we express Eq. (19) in the following manner:

(22)

which can be simplified as:

(23)

Thus, the computation of is not affected by the zero amplitude of . If we consider also that for this particular case the phase of is also zero, then Eq. (23) becomes:

(24)

Therefore, in this case is going to provide the *direction of polarization* of the Love wave, not its direction of propagation. The wave trace is going to be found in the radial component computed with Eq. (17). Now, in the case of real data we can reasonably argue that if for no other reason but for the presence of ambient noise. If in fact this is the case, then Eq.(18) can be used and, along with Eqs.(19) & (20), provides an estimate of the *direction of propagation* of the Love wave. In this case the wave trace is going to be found in the transverse component .

WAVE EXTRACTION USING SYNTHETIC SIGNALS

In this section, we illustrate the application of our proposed procedure to extract waves from synthetic signals. We consider an example very similar to the one presented by Galiana-Merino *et al*. (2011), where a constructed synthetic signal is used. To construct the synthetic signal we combine three windowed sinusoids with frequencies: 5, 2 and 1 Hz, shown in Figure 3, and denoted by , , and , respectively. In order to include elliptically polarized waves, we apply a phase advance of /2 rad to the signal , and a phase delay of /2 rad to the signal . The resulting signals are denoted by and , respectively. The three frequencies are then combined as shown in shown in Figure 4, to obtain a three-component signal, which is simultaneously linearly and elliptically polarized. As Figure 4 indicates, we choose the pro-grade wave of 1 Hz to be in the - plane, with following components: in the -direction, and in the -direction. On the other hand, the retrograde wave of 2 Hz is assigned to the - plane, with the following components: in the -direction and in the -direction. In the *x*-*y* plane we choose to have a linearly polarized wave of 5 Hz defined as in both - and - directions. Since both the and components have the same amplitude, the linearly polarized wave has a direction of propagation of 45 degrees measured clockwise from the positive -axis.

Now, we translate the - - coordinate system into a North-East-Vertical system. For this, we assign an azimuth of 60 degrees (measured clockwise from North) to the retro-grade wave (which propagates along the -axis). Using a right-handed coordinate system, the direction of the other two waves will then be as follows: the azimuth of the pro-grade wave (which propagates along the -axis) will be 150 (=60+90) degrees, and the azimuth of the wave linearly polarized in the *x*-*y* plane will be 105 (=60+45) degrees. We then rotate the *x* and *y* components to obtain the North-East components by means of the rotation matrix:

(25)

The resulting *N*-*E*-*V* components are shown in Figure 5. We can observe the three frequencies are superimposed and there is no visual indication of the type of waves contained in the signal. We will work with these components as starting data for our proposed procedures, since most available seismograms are given in *N*-*E*-*V* components.

Extraction of Retro-grade Rayleigh wave

In this section we will apply filtering to extract the retro-grade wave, that is, the 2-Hz elliptically polarized wave in the *y*-*z* plane. We will use both, the IRE, and independently, the NIP, as criteria to construct and compare the filters. Once the wave is extracted we will recover the azimuth that was assigned to the retro-grade wave in the previous section. We start by computing the Stockwell Transform of the - -*V* components, whose amplitudes are shown in Figures 6(a)-(c). Using the notation introduced in the previous section, , , and . Figures 6(a)-(c) illustrate that, as expected, most of the energy of the linearly polarized wave is contained in the East component, whereas for the elliptical polarized wave, most of the energy is contained in the vertical component. With the Transforms of the *N-E-V* components, and using Eqns. (19)-(21), we compute the angle , shown in Figure 6(d). Because of the color scale distributed in the time-frequency space, we cannot observe exactly the value of the azimuth for each frequency in Figure 6(d), however, we can affirm that the azimuth is close to 100 degrees for the 5 Hz wave (we have assigned 105 degrees in the previous section), 60 degrees for the 2 Hz wave, and 150 degrees for the 1 Hz wave. The exact values of the azimuth for each frequency will be provided after we extract each wave, as it will be shown in the sequel. Now, with the computed angle , we use equation (17) to compute the and components. The results are shown in Figures 6(e)-(f). We can observe that there is no energy in the transverse component for all frequencies. This is an expected result because the angle is derived under the assumption that the correlation between the transverse and vertical components is zero. It is important to clarify that when we compute the component using , each frequency is rotated according to its corresponding . The obtained “radial component” in the full time-frequency space will not have the physical meaning of the Stockwell Transform of a component of the signal in a specific “radial” direction. However, such computation is useful for extracting waves, since after we apply filtering, only one wave (or wave train) will remain in the time-frequency domain, and with it, only one direction of propagation. The next step is the computation of NIP , obtained by applying equation (16) and shown in Figure 7(a). Since we want to extract the wave with retro-grade motion, we set . The red region in Figure 7(a) corresponds to the presence of the retro-grade wave (the NIP), whereas the black region corresponds to the pro-grade wave (the NIP). For the linearly polarized wave, the values of NIP oscillate around zero. This unstable behavior [not shown in figure 7(a)] is due to the presence of the amplitude of in the denominator in Eq. (16); the amplitude of is zero for a wave linearly polarized in the - plane. This situation, however, is unlikely to be found in real seismograms because the presence of noise will keep the amplitude of different from zero. Then, in order to avoid this unstable behavior when dealing with noise-free synthetic signals, the amplitude used in Eq. (16) may be modified in the following manner:

(26)

where is the tolerance for small values of . Because of the finite energy carried by seismic waves, we expect to be bounded. In Figure (7a) the is computed adopting a tolerance . Now, for comparison, the IRE is also shown in Figure 7(b), which was obtained by applying equations (2)-(4). We can observe that the regions corresponding to both the pro-grade and retro-grade wave have an IRE of about 0.5. As expected, the IRE is zero in the region of the linearly polarized wave.

Now that the waves have been identified, we construct filters to isolate or extract the elliptically polarized (retro-grade) wave. The continuous filters based on the NIP and the IRE are constructed as follows:

(27)

where is the threshold value, and the width of the cosine taper. In this example we selected, , , and to construct the filter using as criterion the value of the IRE. On the other hand, for the filter using as criterion the value of the NIP, we selected , , and . Since we already computed the component , the filters can be applied to it, and to the vertical component to extract directly the Rayleigh waves. In Figures 7(c)-(d) we compare the filtered component using the NIP criterion [Figure 7(c)], and the IRE [Figure 7(d)]. It is evident that filtering with the IRE criterion alone does not separate the pro-grade and retro-grade waves in this example. On the other hand, Figure 7(c) shows the effectiveness of the NIP criterion to isolate the retro-grade (Rayleigh) waves present in the synthetic signals.

Finally, the desired wave is extracted by computing the inverse Stockwell transforms after the , and components are filtered with the NIP criterion. Figure 8 shows the radial, transverse and vertical components of the unfiltered signal and those of the extracted wave in the time domain. In the previous section we selected the *y*-axis as the direction of propagation of the retro-grade wave, and thus, the *y*-axis is the “radial” direction for this wave. As expected, there is no extracted wave in the transverse direction (the pro-grade wave which would have appeared on the transverse component has been eliminated by filtering).

Let us note that we use to compute the NIP , and then we use the NIP to *filter* and *extract* the desired wave. However, even though the components of the extracted wave are already obtained in the radial and transverse direction, the unique numerical value giving the azimuth of such directions has not been provided. If such azimuth is also desired, it can be computed by filtering the , and components with the NIP criterion. Then, the angle is computed using Eqs. (10)-(12) once the time-domain *N-E-V* components are obtained inverting the filtered , and components. The *N-E-V* components of the extracted retro-grade wave computed in this manner are shown in Figure 9. The extracted wave has a frequency of 2 Hz, as expected. Now, applying Eqs. (10)-(12) to these *N-E-V* components, we obtain an azimuth for the retro-grade Rayleigh wave of 59.9994 degrees, the expected value. Let us note that the *R-T-V* components of Figures 8(d)-(f) were obtained by rotating the *N-E-V* components of Figure 5 with the computed azimuth.

Extraction of Pro-grade Rayleigh Wave

To extract the pro-grade Rayleigh wave from the synthetic signal we follow the same procedure as in the previous section, but now we set , for a phase delay for the vertical component We can observe in Figure 10(a) that the regions for the NIP and the NIP have been interchanged [compare Figure 10(a) with Figure 7(a)], since now we are targeting the wave of 1 Hz (which, we remind the reader, is the pro-grade wave propagating along the *x*-axis, that is, an azimuth of 150 degrees). When we apply the filter, based on the NIP criterion, to the component, we can observe that the only remaining wave has a frequency of about 1 Hz, as shown in Figure 10(b). Finally, the radial, transverse and vertical component of the unfiltered signal and extracted wave are shown in Figure 11. Once again, there is no component in the “transverse” direction of the extracted wave. The azimuth giving the direction of propagation of the pro-grade wave, obtained by applying Eqs. (10)-(12) is 150.0011 degrees. As expected, in this case the “radial” direction coincides with the *x*-axis of the coordinate system, as shown in Figure 11.

To verify that we in fact have extracted retro-grade and pro-grade Rayleigh waves, we inspect their polarization characteristics. In Figure (12) we compare the radial and shifted vertical components of the extracted waves. For the retro-grade, the vertical component is shifted with a phase advance, and for the pro-grade wave, with a phase delay. Since the compared components are clearly in-phase, we can conclude that we have extracted Rayleigh waves.

Extraction of Linearly Polarized wave

Now we consider the problem of extracting the wave that is linearly polarized in the - plane. In such a case, Love waves and shear waves would be the candidates. For Love waves we would expect the presence of a dispersed wave train. Note that to extract the linearly polarized wave, the component can be obtained either way, by shifting with a phase advance, or a phase delay. In Figure (13a) the was computed shifting with a phase delay. We can observe that the values of the for the 5 Hz wave are close to zero, a result consistent with linear polarization. Thus, in this case the continuous filter is constructed to exclude regions of the plane for which , as follows:

$$- \quad \frac{\quad}{\quad} \quad - \tag{28}$$

where , and . The results of applying this filter to the component are shown in Figure (13b). It can be observed that the only remaining wave in the filtered component is the wave of 5 Hz. Next, the radial, transverse and vertical components of the unfiltered signal and extracted wave are shown in Figure (14). Here the *y*-*x* components of the unfiltered signal have been rotated 45 degrees, to obtain its radial and transverse components. Even before filtering we can already observe that the high frequency wave is present only in the “radial component. Regarding the extracted wave, Figure (14) shoes that only the radial component of the extracted signal is non-zero, consistent with what it was anticipated. Now, in this case of a noise-free synthetic signal, Eq. (10) is not appropriate to compute the azimuth of the direction of polarization of the wave, since the time-domain component is zero. However, we can take advantage of the fact that we have already extracted the radial component of the wave. Let us note that for a wave linearly polarized on the horizontal plane:

(29)

if is in the direction of polarization. Thus, a new expression can be obtained, in the same manner we derived Eq. (10):

(30)

After computing the North and East components of the extracted wave (inverting the filtered and components) the azimuth obtained using Eqs. (30) and (12) is 105.0004. It is important to remark that this azimuth gives the direction of polarization. If the extracted wave is a Love wave, its direction of propagation would be perpendicular to it.

AN EXAMPLE WITH REAL SIGNALS

In this section we apply the procedure for identification and extraction of surface waves produced by an aftershock of the Chi-Chi earthquake in the West Coastal Plain (WCP) in Taiwan, which occurred on

September, 20th 1999 at 1803 UTC with a magnitude of M*w* 6.2. This aftershock is very useful to test the proposed method to extract surface waves, since it produced very strong and clear surface waves in the WCP. Besides, since Rayleigh and Love waves had been previously identified from the recordings and reported in the literature (*e.g.*, Wang *et al.*, 2006) this data set allows us to assess with confidence if we are in fact extracting Rayleigh and Love waves. Figure (15) shows a map with the directions of the Rayleigh wave propagation obtained by Wang *et al.* (2006), where the location of the epicenter is also indicated. The circle in Figure (15) specifies the location of station TCU116, which we will consider for this example.

Extraction of Retro-grade Rayleigh waves

The *N-E-V* components of the displacement time history at station TCU116 during the aftershock are shown in Figure (16). The displacements were obtained by independently bandpass filtering between 0.1 and 10 Hz and integrating twice the components of the acceleration histories. We can observe from the time histories in Figure (16) that most of the energy of the signal is contained in the East and Vertical components. The Stockwell Transforms of the displacements histories are computed, and with them, we compute the angle using Eqs. (19)-(20). Then, the components and are computed according to Eq. (17). The results are shown in Figure (17). In Figure 17(a) we can observe regions in the time-frequency domain (between 20 and 50 seconds) with small variations of the values of , which can be associated to wave trains. We find very little energy in the component, even in this case of a real signal, since is derived under the assumption of zero correlation between the and components. The next step is the computation of NIP , obtained by applying equation (16) and shown in Figure 18(a). Since we want to extract Rayleigh waves with retro-grade motion first, . Figure 18(a) shows that using the NIP we can identify the regions of the plane where the components and are best correlated. The region corresponding to the retro-grade motion is indicated by the red color. For comparison, the IRE is also shown in Figure 18(b). We can conclude from the comparison that the NIP is more stable over the domain, as opposed to the IRE, which has more variation in the Stockwell transform domain. In Galiana-Merino *et al*. (2011), it is even stated that a 2D filter needs to be applied to the IRE obtained with the SWPD, because its high variation could lead to numerical problems. In this example, since we are not dealing with synthetic signals, the NIP is computed with Eq. (16) without making any modification to , and without any smoothing.

Figure 18(c) shows the component filtered with the NIP criterion, according to Eq. (27). The same component filtered with the IRE criterion is shown in Figure 18(d). The results of this example clearly demonstrate that filtering with the NIP criterion effectively isolates the retro-grade wave from the pro-grade wave. Upon inverting the filtered transforms, we obtain the extracted retro-grade wave. In Figure (19) we can observe the radial, transverse and vertical components of the unfiltered signal and the extracted retro-grade wave. The comparison between the unfiltered signal and extracted wave shows that filtering has excluded a wave component observed between 25 and 35 seconds. Such component would not have been excluded filtering with the IRE criterion alone. We can also observe that the transverse component of the extracted wave is minimized. The correlation coefficient computed as in Eq. (5) between the radial and shifted (with a phase advance) vertical components of the extracted wave is 0.91097, showing in a quantitative manner the good results that are obtained when the NIP criterion is used. Finally, the azimuth of the direction of propagation of the Rayleigh wave is computed with Eqs. (10)-(12), obtaining a value of 257.9926 degrees. This result is compatible with the directions reported by Wang *et al*. (2006), indicated in Figure (15). The angle of

257.9926 degrees was used to rotate the *N-E-V* components of the unfiltered signal to obtain the components *R-T-V* components shown in Figures 19(a)-(c).

Extraction of Pro-grade Rayleigh waves

Figure 20(a) shows NIP to extract the pro-grade Rayleigh waves, and Figure 20(b) shows the component when filtered with this criterion. We observe that the pro-grade wave train has different frequency content (higher frequencies) than that of the retro-grade wave train, and that it is located at around 30 seconds. Figure 21 shows the radial, transverse, and vertical components of the unfiltered signal and extracted pro-grade wave. We can observe the different time location of the pro-grade wave relative to the previously extracted retro-grade wave. With the use of the NIP criterion, we have managed to separate these waves, even in the time range in which they overlap. Certainly, such separation is possible because of the different frequency content of the waves. The correlation coefficient of the radial and shifted (with a phase delay) vertical components of the extracted pro-grade wave is 0.91034. The computed azimuth is 282.6976 degrees. This azimuth is significantly different from the one obtained for the retro-grade waves (257.9926 degrees), indicating that probably the observed pro-grade and retro-grade Rayleigh waves are generated in different manners.

Finally Figure (22) shows the comparison between the radial and shifted vertical components of the extracted Rayleigh waves. Clearly, the radial component and the vertical component shifted with a phase advance shown in Figure 22(a) are in phase, confirming the extracted waves of Figure 22(a) are retro-grade Rayleigh waves. In Figure 22(b) the vertical component is shifted with a phase delay, confirming that the extracted wave shown in Figure 22(b) is a pro-grade Rayleigh wave.

Extraction of Love waves

In Figure (17) we can observe that the component at station TCU116 does not show the presence of a wave train that can be associated to Love waves. This is why we analyze the recording of the same event at station TCU118, for which Wang *et al*. (2006) had already identified Love waves. For this station we first extract the retro-grade Rayleigh wave train, following the procedure detailed in the previous section. The components of the extracted retro-grade Rayleigh wave are shown in Figure 23(a). Let us note that the resulting azimuth giving the direction of propagation of the retro-grade Rayleigh wave train is 304.51 degrees, a result close to the 297 degrees reported in Wang *et al*. (2006). With this direction we use Eq. (7) to compute the radial and transverse components of the unfiltered signal in the time domain, and then compute their Stockwell Transforms, which are shown in Figure (24). A wave train with a later arrival time (relative to the Rayleigh wave's arrival) is clearly present in the time-frequency transverse component of the unfiltered signal, as shown in Figure 24(b). The Love waves are effectively extracted using the filter based on the criterion defined in Eq. (27). Even though we could use the criterion and construct a filter according to Eq. (28), the filter given in Eq. (23) is more convenient because the is more stable in the space. The extracted Love waves are shown in Figure 23(b). The waveforms and corresponding arrival times of the waves extracted with our proposed procedure are similar to those reported in Figure 9 of Wang *et al*., (2006).

Now, to illustrate the performance of our procedure to extract surface waves in high noise conditions, we analyze the recording at station CHY107. This station is located farther from the epicenter, to the south of the WCP, as shown in Figure 15. The strength of the wavefield at such far location is weak. A comparison of the unfiltered signal and the results of applying filtering using the NIP criterion are shown in Figure 25. We can observe that much of the noise has been filtered out when the NIP criterion is used. The correlation coefficient between the radial and shifted vertical components is 0.8449, giving a strong indication that the extracted (retro-grade) wave in the radial direction is a Rayleigh wave. This high correlation is illustrated in Figure 25(d), which shows the comparison of the radial and phase advanced vertical component. Furthermore, the azimuth obtained with the extracted waves is 226.22 degrees, a direction consistent with the location of station CHY107 relative to the epicenter, shown in Figure 15. We can also observe a strong intensity (relative to the radial component) in the transverse component of the extracted waves. Even though we could consider the extracted waves in this transverse component as Love waves, the extracted signal might as well be simply linearly polarized noise. In cases like this, with a relatively lower signal-to-noise ratio, better results can be obtained if the signal is denoised before applying filtering to extract Love waves.

Finally, we have applied the NIP criterion to extract Rayleigh and Love waves to other stations at the WCP in Taiwan. Figure 26 illustrates the extracted retro-grade and pro-grade Rayleigh waves at each station. The Love waves, extracted from the transverse component of the retro-grade Rayleigh waves are shown in Figure 27. The results show the extraction method is stable when applied to this dataset of seismic time histories. The computed azimuths of retro-grade Rayleigh wave propagation are in excellent agreement with those obtained by Wang *et al*. (2006), indicated in Figure (15).

CONCLUSIONS

We have proposed and developed a method to extract Rayleigh and Love waves from three-component displacement histories. The proposed method, based on the Normalized Inner Product (NIP), does not require *a priori* estimations of the frequency range and direction of propagation of the surface waves. We have shown that the method proposed herein distinguishes between pro-grade and retro-grade particle motion. Therefore surface waves with such different polarization characteristics can be more easily identified. Furthermore, examples with real signals show that the Normalized Inner Product is more stable over the time-frequency domain than the Instantaneous Reciprocal Ellipticity. We also showed that the proposed method works well for extracting Love waves from noise-free synthetic seismograms as well as from real seismograms. The method was applied to extract Rayleigh and Love waves from displacement histories of aftershock 1803 of the Chi-Chi earthquake recorded at the Western Coastal Plain in Taiwan. The extracted waves and corresponding directions of propagation are in excellent agreement with previous surface wave analysis reported in the literature.

DATA AND RESOURCES

All recorded seismograms used in this work are from CD-002 titled "CWB Free-Field Strong-Motion Data from Three Major Aftershocks of the 1999 Chi-Chi Earthquake: Processed Acceleration Data Files on CD-ROM" prepared in 2001 by W. H. K. Lee, T. C. Shin, and C. F. Wu of the Seismological Observation Center, Central Weather Bureau, Taiwan.

The relief geographic map of the West Coastal Plain was generated with the code READHGT written by François Beauducel, from the Institute de Physique du Globe de Paris. Input data for the Digital Elevation Map was downloaded from http://dds.cr.usgs.gov/srtm/version2_1. Coast lines were extracted from http://www.ngdc.noaa.gov/mgg/coast/getcoast.html. Both websites were last accessed in January 2014.

ACKNOWLEDGEMENTS

The authors are grateful to two anonymous reviewers for constructive comments which improved the clarity of the manuscript. The authors are also indebted to Dr. Fabian Bonilla for fruitful discussions on surface wave propagation, and for introducing us to the use of the Stockwell transform for analysis of non-stationary signals.

This research has been co-financed by Electricité de France (EDF) through the MARS project and by the European Union (European Social Fund – ESF) and Greek national funds through the Operational Program "Education and Lifelong Learning" of the National Strategic Reference Framework (NSRF) - Research Funding Program: **THALES**. Investing in knowledge society through the European Social Fund.

REFERENCES

Baker, G.E. and Stevens, J.L. (2004). "Backazimuth estimation reliability using surface wave polarization", *Geophysical Research Letters*, **31**, L09611, doi:10.1029/2004GL019510.

Chael, E.P. (1997) "An automated Rayleigh-wave detection algorithm", *Bull. Seism. Soc. Am.* **87**, 157–163.

Dziewonski, A., Bloch, S. and Landisman, M. (1969) "A Technique for the Analysis of Transient Seismic Signals", *Bull. Seismol. Soc. Am.*, **59**(1), 427-444.

Flinn, E.A. (1965) "Signal analysis using rectilinearity and direction of particle motion", *Proc. IEEE*, **53**, 1874–1876.

Galiana-Merino J.J., Parolai, S., and Rosa-Herranz, J. (2011). "Seismic wave characterization using complex trace analysis in the stationary wavelet packet domain", *Soil Dynamics and Earthuqake Engineering*. **31**(11), 1565–1578.

Li, X.L., Crampin S. (1991) "Complex component analysis of shear wave splitting: theory", *Geophysical Journal International*. **107**, 597-604.

Pinnegar, C.R. (2006). "Polarization Analysis and polarization filtering of three-component signals with the time-frequency S transform", *Geophysical Journal International*. **165**, 596–606.

René, R.M., Fitter, J.L., Forsyth, P.M., Kim K.Y., Murray, D.J., Walters, J.K. (1986) "Multicomponent seismic studies using complex trace analysis", *Geophysics*. **51**, 1235-1251.

Selby, N.D. (2001) "Association of Rayleigh waves using back-azimuth measurements: application to Test Ban verification", *Bull. Seism. Soc. Am*. **91**, 580–593.

Smart, E. (1978) "A Three-Component, Single-Station, Maximum-Likelihood Surface Wave Processor", *Seismic Data Analysis Center Report*, SDAC-TR-77-14, 62 pp.

Stockwell, R.G. (2007) "Why use the S-transform" in *Pseudo-Differential Operators: PDEs and Time-Frequency Analysis*. (Fields Institute Communications), **52**, pp. 279–309.

Stockwell, R., Mansinha, L., Lowe, R. (1996) "Localization of the Complex Spectrum: The S Transform", *IEEE Transactions on Signal Processing.* **44** (4), 998–1001.

Vidale, J.E., (1986) "Complex polarization analysis of ground motion", *Bull. Seismol. Soc. Am.*, **76**(5), 1393-1405.

Wang, G., Tang, G., Boore, D., Burbach, G., Jackson, C., Zhou, X., and Lin, Q. (2006). "Surface Waves in the Western Taiwan Coastal Plain from an Aftershock of the 1999 Chi-Chi, Taiwan, Earthquake", *Bull. Seism. Soc. Am.* **96**, 821-845.

AUTHORS' AFFILIATIONS:

[1] Universidad Nacional Autónoma de Honduras, Tegucigalpa, Honduras. E-mail: kristelmeza@unah.edu.hn

[2] Department of Civil Engineering, University of Patras, GR-26500 Patras, Greece. E-mail: papaga@upatras.gr

[3] Université Paris-Est, IFSTTAR, Départ. GERS, 20 Boulevard Newton, Champs sur Marne, France. E-mail: jean-francois.semblat@ifsttar.fr.

FIGURE CAPTIONS

Figure 1. Time shift for vertical component. (a) For pro-grade motion (phase delay) (b) For retro-grade motion (phase advance).

Figure 2. Reference system for direction of propagation of Rayleigh waves.

Figure 3. Windowed sinusoids to construct synthetic signal. (a) : 5 Hz, (b) : 1 Hz, (c) :2 Hz.

Figure 4. Three-component synthetic signal. (a) − , (b) − , (c) .

Figure 5. Three-component synthetic signal. (a) North component, (b) East component, (c) Vertical component.

Figure 6. Time-frequency representation of synthetic signal. (a) Amplitude of North component, (b) Amplitude of East component, (c) Amplitude of vertical component, (d) Azimuth of direction of propagation according to Eq. (20), (e) Amplitude of radial component (f) Amplitude of transverse component.

Figure 7. Comparison of filtering using the IRE and NIP criteria. (a) Normalized inner product of radial and phase advanced vertical component, (b) IRE computed with the three-components of the signal, (c) Radial displacement component filtered using the NIP criterion, (d) Radial displacement component filtered using the IRE criterion.

Figure 8. Rayleigh retro-grade wave extracted from synthetic signal. (a) Unfiltered transverse (-) component, (b) Unfiltered radial (-) component, (c) Unfiltered (-) vertical component, (d) Extracted transverse component, (e) Extracted radial component, (f) Extracted vertical component.

Figure 9. Extracted retro-grade Rayleigh wave. (a) North component, (b) East component, (c) Vertical component.

Figure 10. Extraction of pro-grade wave using the NIP criterion. (a) Normalized inner product of radial and phase delayed vertical component, (b) Amplitude of component filtered with the NIP criterion.

Figure 11. Rayleigh pro-grade wave extracted from synthetic signal. (a) Unfiltered radial (-) component, (b) Unfiltered transverse (-) component, (c) Unfiltered (-) vertical component, (d) Extracted radial component, (e) Extracted transverse component, (f) Extracted vertical component.

Figure 12. Comparison of radial and shifted vertical components of extracted waves. (a) Retro-grade wave (2 Hz), (b) Pro-grade wave (1 Hz).

Figure 13. Extraction of linearly polarized wave using the NIP criterion. (a) Normalized inner product of radial and phase delayed vertical component, (b) Amplitude of component filtered with the NIP criterion.

Figure 14. Linearly polarized wave extracted from synthetic signal. (a) Unfiltered radial component, (b) Unfiltered transverse component, (c) Unfiltered vertical component, (d) Extracted radial component, (e) Extracted transverse component, (f) Extracted vertical component.

Figure 15. Map illustrating the location of the stations on the West Coastal Plain considered in this study. For some stations the arrows indicate the direction Rayleigh wave propagation estimated by Wang *et al*. (2006). The star indicates the location of the epicenter of the event. The black circle indicates the location of station TCU116.

Figure 16. *N-E-V* components of the displacement history (in cm) for Chi-Chi aftershock 1803 at station TCU116. (a) North component (b) East component (c) Vertical component.

Figure 17. Radial and Transverse displacement components for the NIP at station TCU116. (a) Azimuth of direction of propagation, (b) Amplitude of component (c) Amplitude of component.

Figure 18. Comparison of filtering to extract the retro-grade wave from recording at station TCU116 using the IRE and NIP criteria. (a) Normalized inner product of and phase advanced component, (b) IRE computed with the three-components of the signal, (c) component filtered with the NIP criterion, (d) component filtered with the IRE criterion.

Figure 19. Rayleigh retro-grade wave extracted at station TCU116. (a) Unfiltered radial component, (b) Unfiltered transverse component, (c) Unfiltered vertical component, (d) Extracted radial component, (e) Extracted transverse component, (f) Extracted vertical component.

Figure 20. Extraction of pro-grade Rayleigh wave from recording at station TCU116. (a) Normalized inner product of and phase delayed component, (b) Amplitude of component filtered with the NIP criterion.

Figure 21. Rayleigh pro-grade wave extracted at station TCU116. (a) Unfiltered radial component, (b) Unfiltered transverse component, (c) Unfiltered vertical component, (d) Extracted radial component, (e) Extracted transverse component, (f) Extracted vertical component.

Figure 22. Comparison of radial and shifted vertical components of extracted Rayleigh waves at station TCU116. (a) Retro-grade wave, (b) Pro-grade wave.

Figure 23. *R*-*T*-*V* displacement components of extracted waves at station TCU118. (a) Comparison of radial and shifted vertical component of retro-grade Rayleigh wave (b) Extracted (Love) wave in transverse direction.

Figure 24. Radial and Transverse time-frequency components for unfiltered recording at station TCU118. (a) Amplitude of radial component (b) Amplitude of transverse component.

Figure 25. Extracted waves from recording at station CHY107. (a) Unfiltered radial component, (b) Unfiltered transverse component, (c) Unfiltered vertical component, (d) Extracted radial component (black line) and shifted vertical component (gray line), (e) Extracted transverse component, (f) Extracted vertical component.

Figure 26. Radial component (black solid line) and shifted vertical component (gray dashed line) of extracted Rayleigh waves at different stations of the WCP plain in Taiwan. (a) Retro-grade waves, (b) Pro-grade waves.

Figure 27. Extracted Love waves at different stations of the WCP plain in Taiwan.

FIGURES

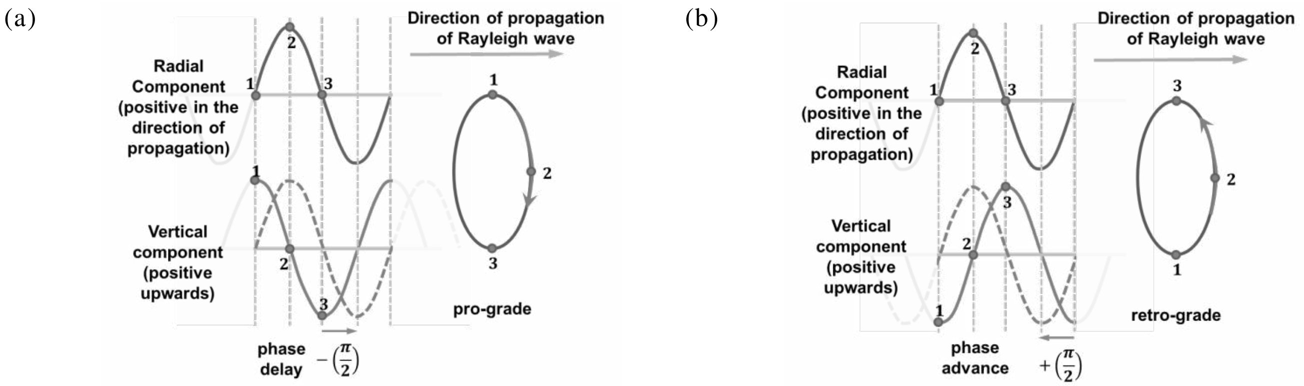

Figure 1. Time shift for vertical component. (a) For pro-grade motion (phase delay) (b) For retro-grade motion (phase advance)

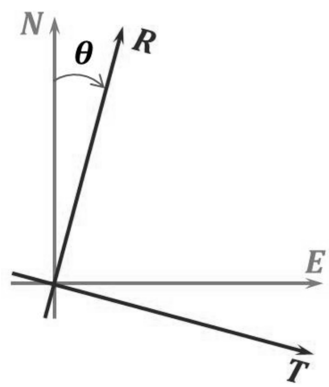

Figure 2. Reference system for direction of propagation of Rayleigh waves.

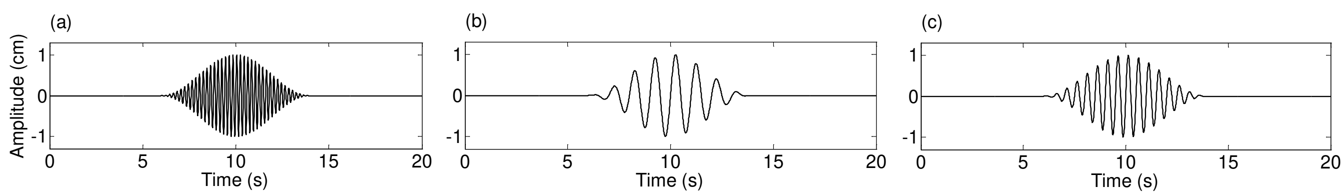

Figure 3. Windowed sinusoids to construct synthetic signal. (a) : 5 Hz, (b) : 1 Hz, (c) :2 Hz.

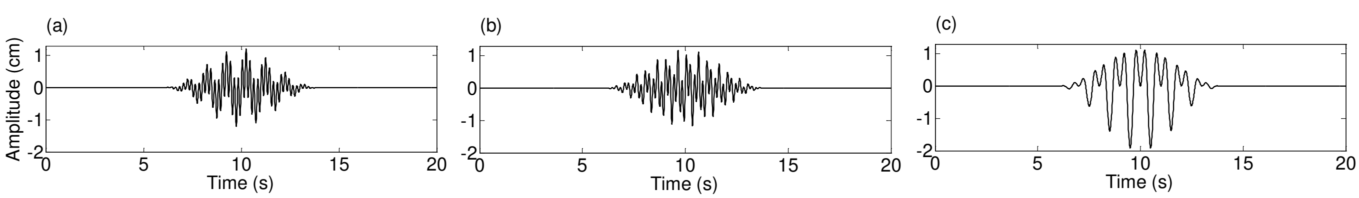

Figure 4. Three-component synthetic signal. (a) , (b) , (c) .

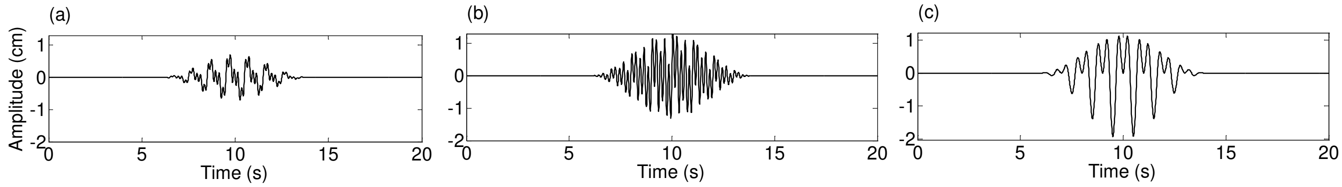

Figure 5. Three-component synthetic signal. (a) North component, (b) East component, (c) Vertical component.

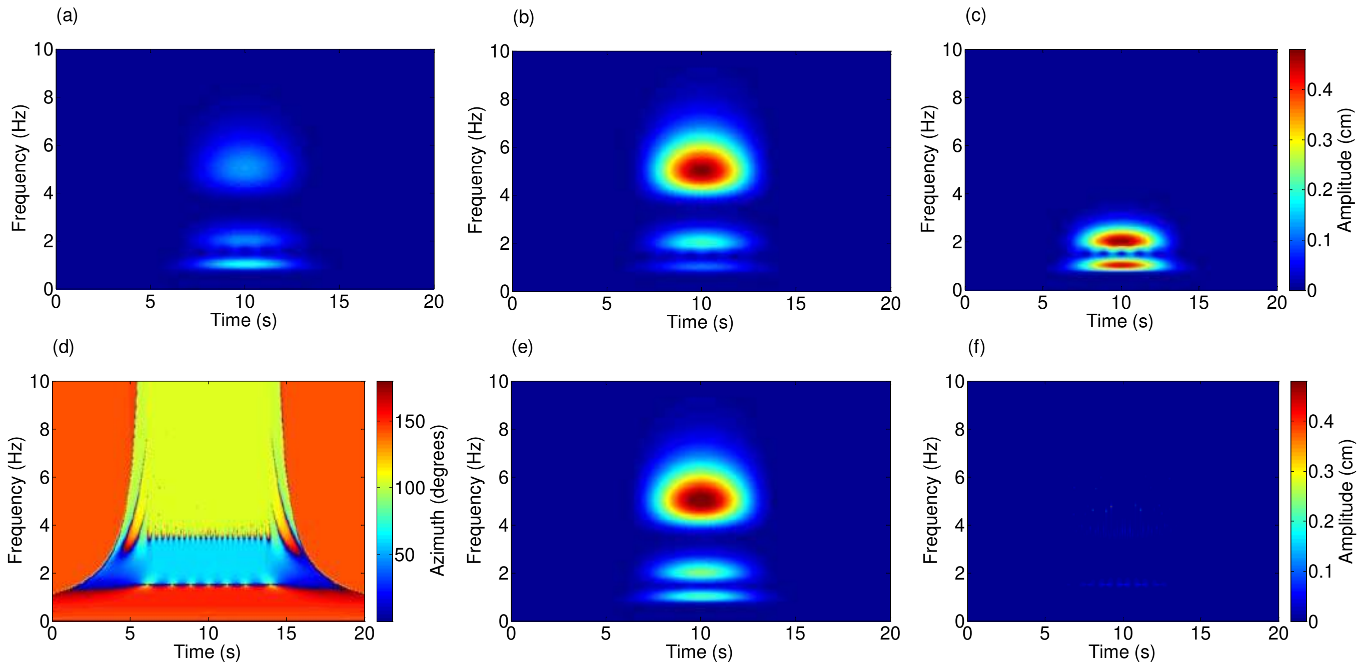

Figure 6. Time-frequency representation of synthetic signal. (a) Amplitude of North component, (b) Amplitude of East component, (c) Amplitude of vertical component, (d) Azimuth of direction of propagation according to Eq. (20), (e) Amplitude of radial component (f) Amplitude of transverse component.

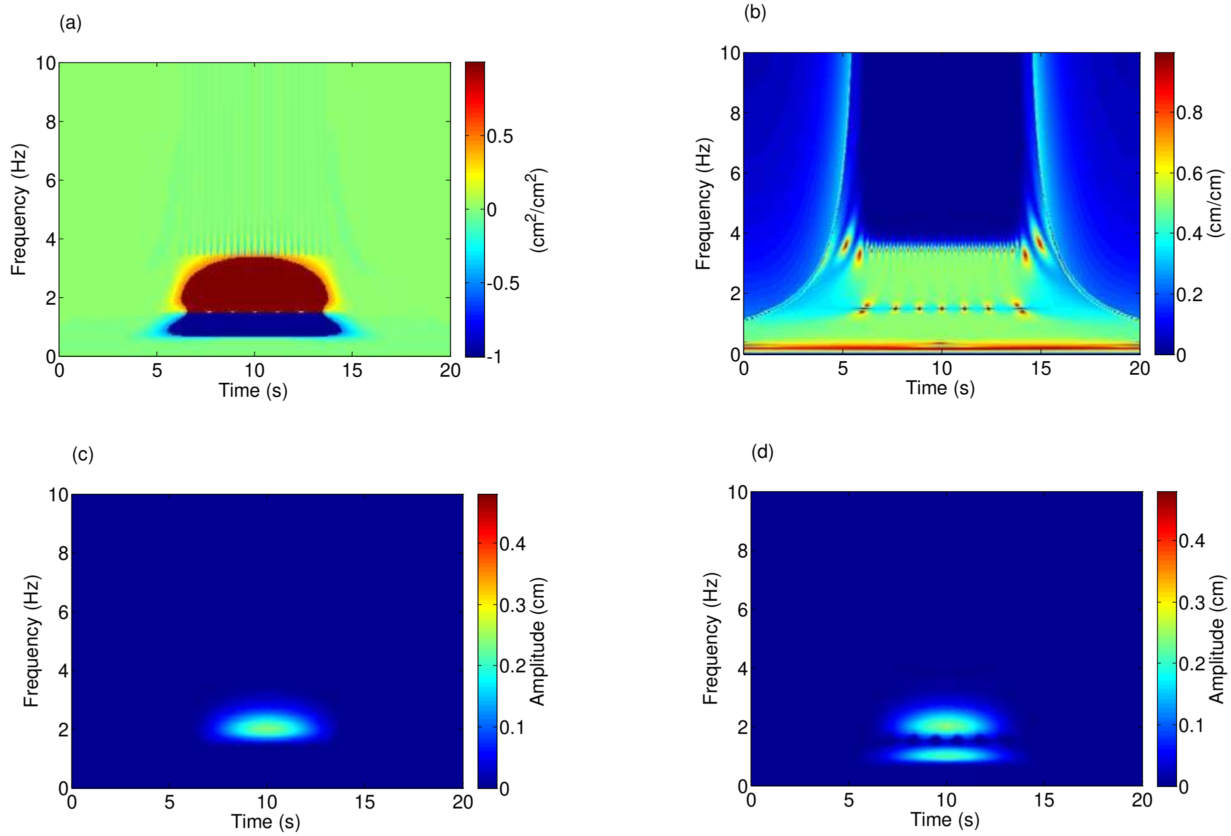

Figure 7. Comparison of filtering using the IRE and NIP criteria. (a) Normalized inner product of radial and phase advanced vertical component, (b) IRE computed with the three-components of the signal, (c) Radial displacement component filtered using the NIP criterion, (d) Radial displacement component filtered using the IRE criterion.

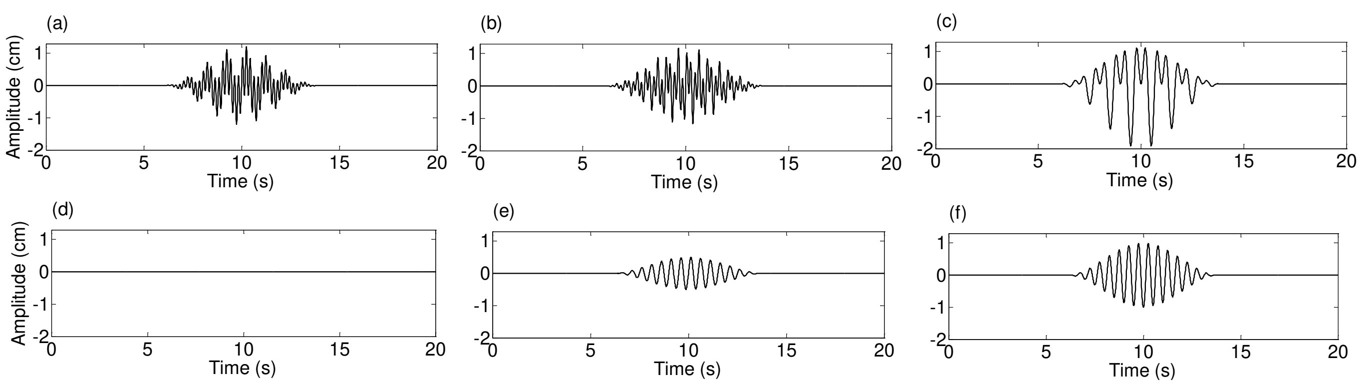

Figure 8. Rayleigh retro-grade wave extracted from synthetic signal. (a) Unfiltered transverse (-) component, (b) Unfiltered radial (-) component, (c) Unfiltered (-) vertical component, (d) Extracted transverse component, (e) Extracted radial component, (f) Extracted vertical component.

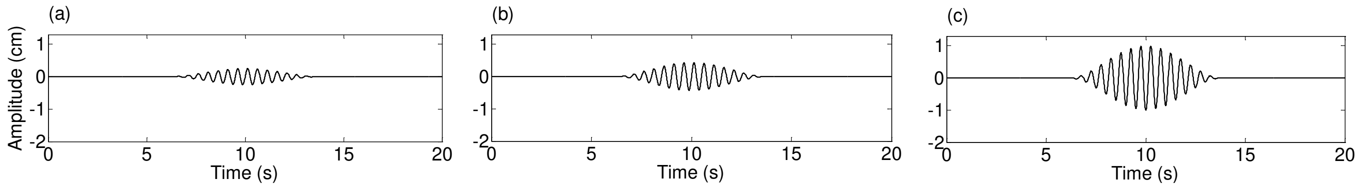

Figure 9. Extracted retro-grade Rayleigh wave. (a) North component, (b) East component, (c) Vertical component.

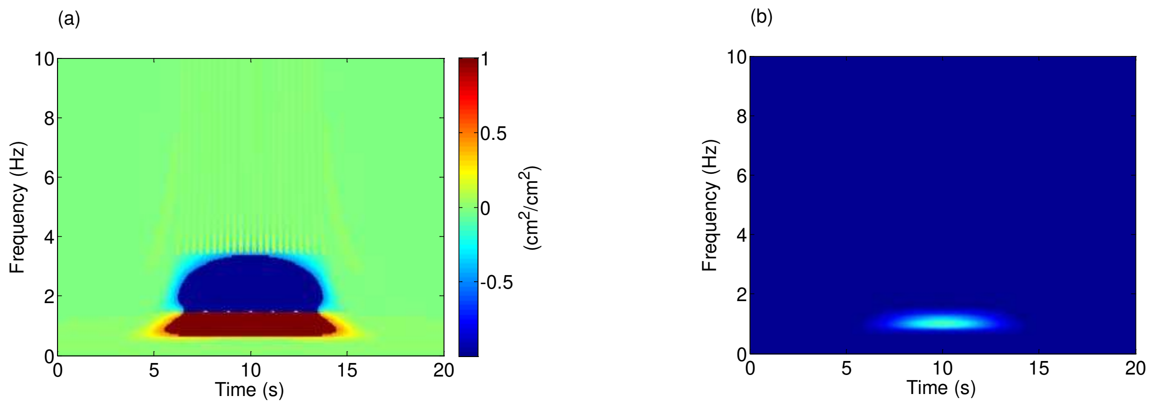

Figure 10. Extraction of pro-grade wave using the NIP criterion. (a) Normalized inner product of radial and phase delayed vertical component, (b) Amplitude of component filtered with the NIP criterion.

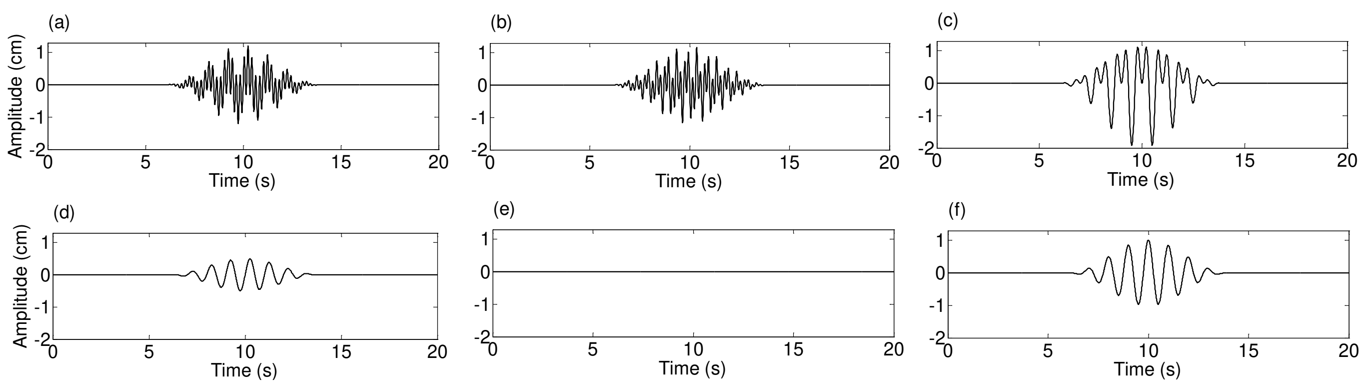

Figure 11. Rayleigh pro-grade wave extracted from synthetic signal. (a) Unfiltered radial (-) component, (b) Unfiltered transverse (-) component, (c) Unfiltered (-) vertical component, (d) Extracted radial component, (e) Extracted transverse component, (f) Extracted vertical component.

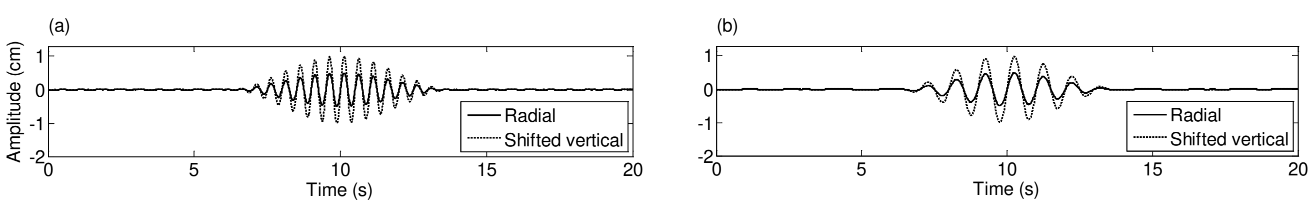

Figure 12. Comparison of radial and shifted vertical components of extracted waves. (a) Retro-grade wave (2 Hz), (b) Pro-grade wave (1 Hz).

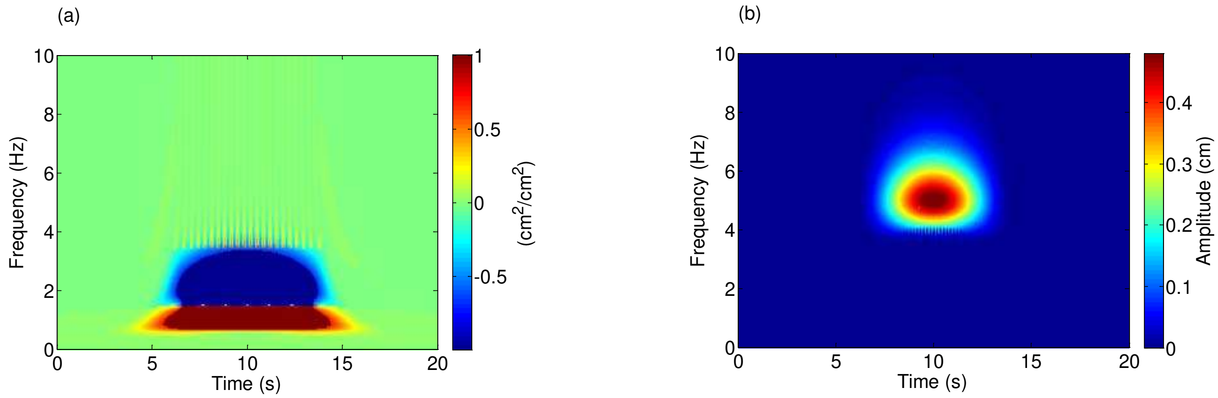

Figure 13. Extraction of linearly polarized wave using the NIP criterion. (a) Normalized inner product of radial and phase delayed vertical component, (b) Amplitude of component filtered with the NIP criterion.

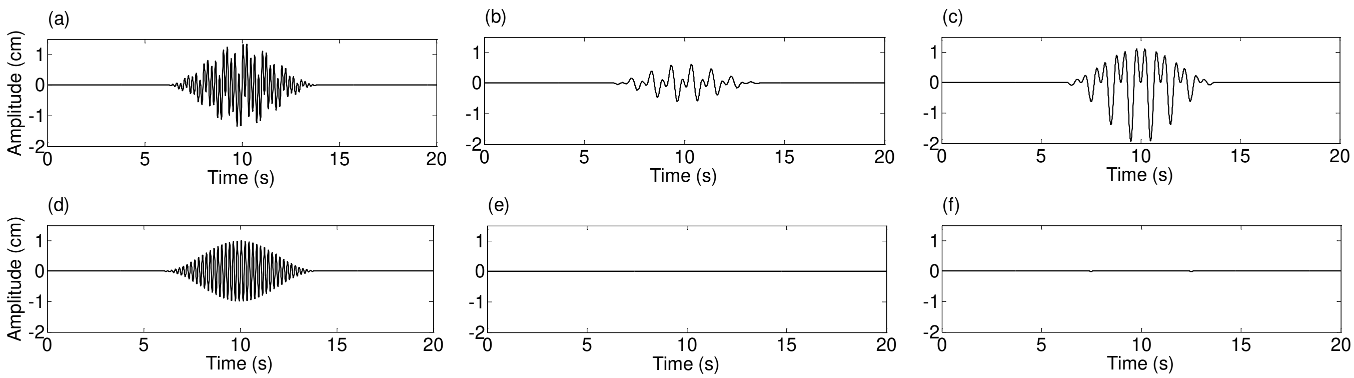

Figure 14. Linearly polarized wave extracted from synthetic signal. (a) Unfiltered radial component, (b) Unfiltered transverse component, (c) Unfiltered vertical component, (d) Extracted radial component, (e) Extracted transverse component, (f) Extracted vertical component.

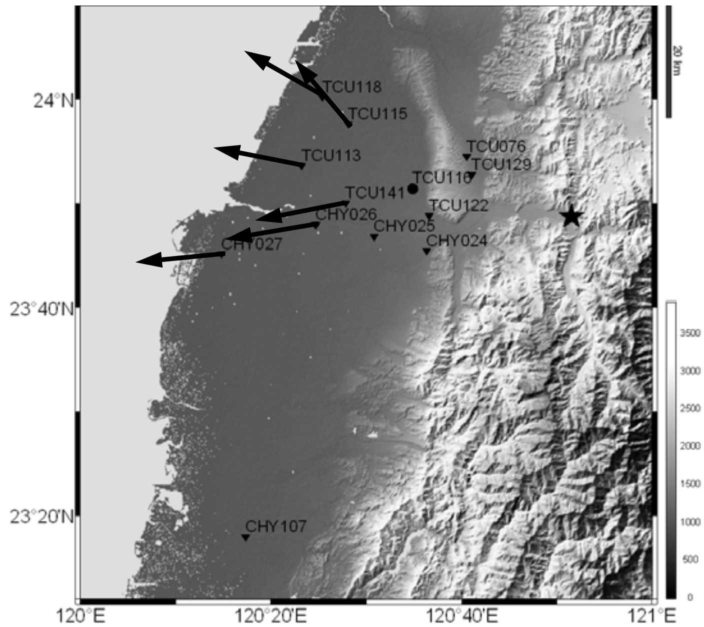

Figure 15. Map illustrating the location of the stations on the West Coastal Plain considered in this study. For some stations the arrows indicate the direction Rayleigh wave propagation estimated by Wang *et al*. (2006). The star indicates the location of the epicenter of the event. The black circle indicates the location of station TCU116.

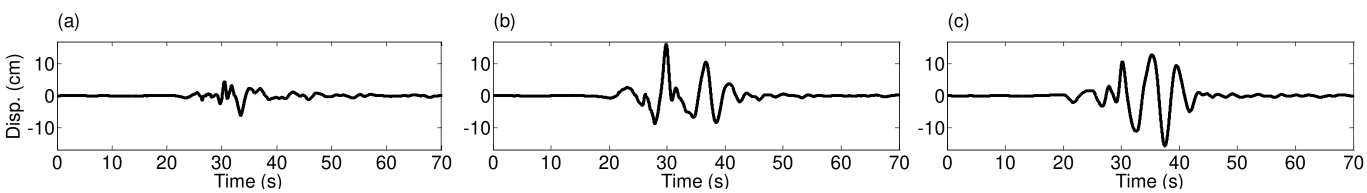

Figure 16. *N-E-V* components of the displacement history (in cm) for Chi-Chi aftershock 1803 at station TCU116. (a) North component (b) East component (c) Vertical component.

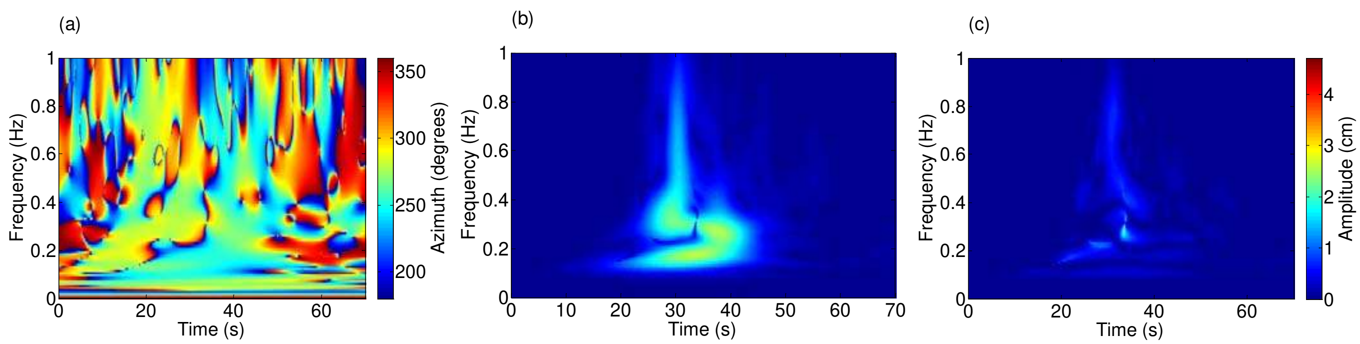

Figure 17. Radial and Transverse displacement components for the NIP at station TCU116. (a) Azimuth of direction of propagation, (b) Amplitude of component (c) Amplitude of component.

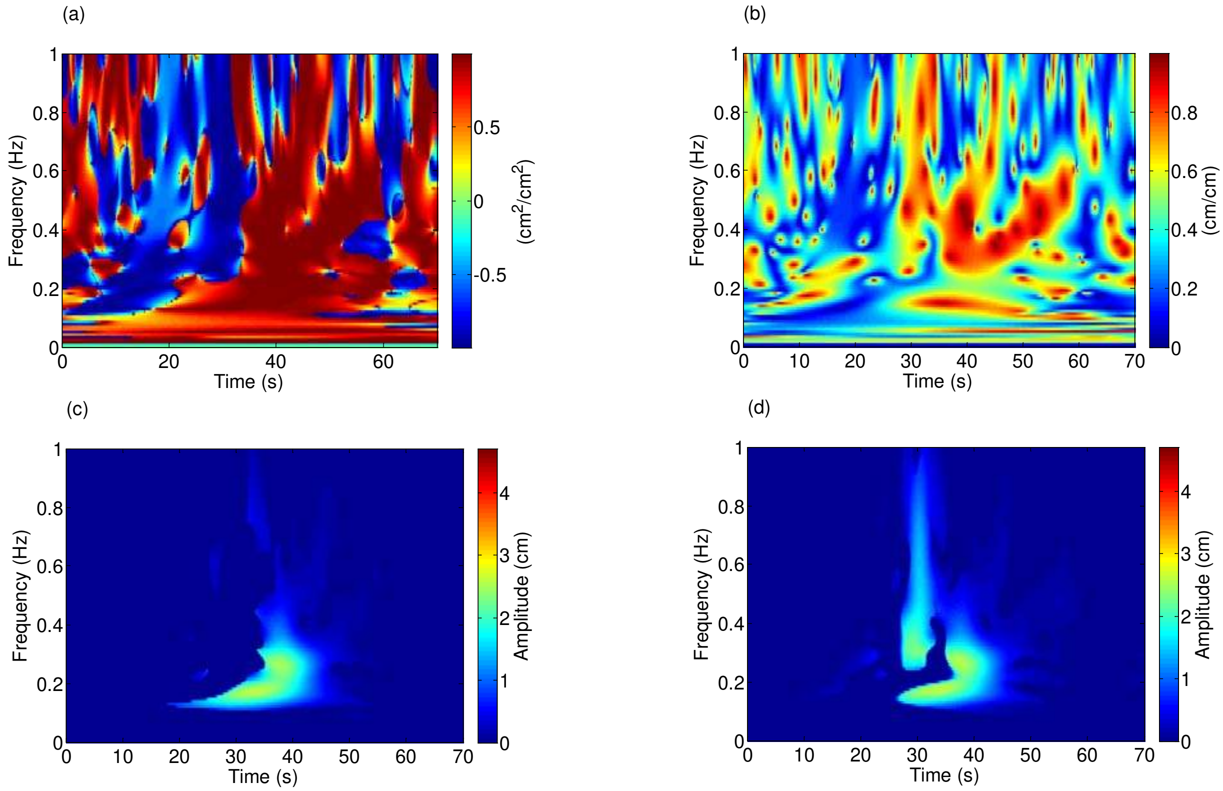

Figure 18. Comparison of filtering to extract the retro-grade wave from recording at station TCU116 using the IRE and NIP criteria. (a) Normalized inner product of and phase advanced component, (b) IRE computed with the three-components of the signal, (c) component filtered with the NIP criterion, (d) component filtered with the IRE criterion.

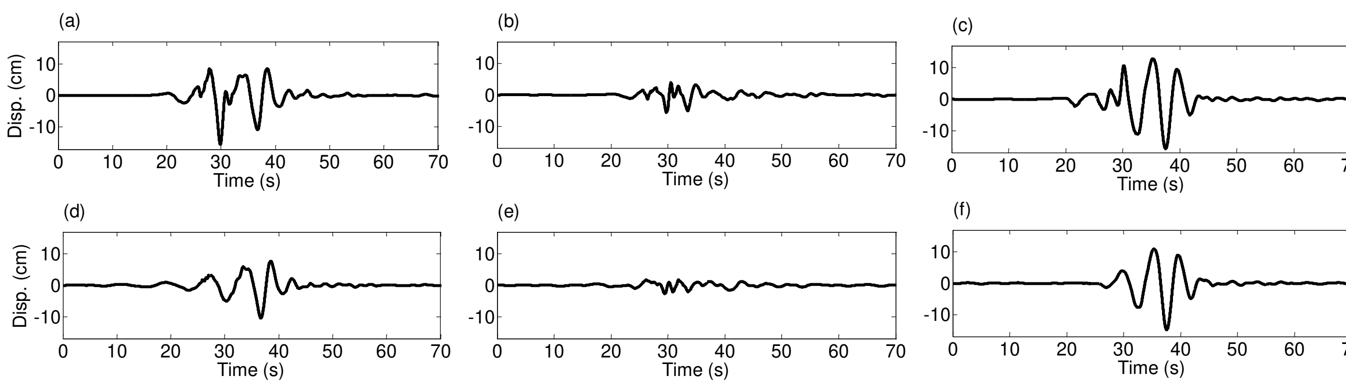

Figure 19. Rayleigh retro-grade wave extracted at station TCU116. (a) Unfiltered radial component, (b) Unfiltered transverse component, (c) Unfiltered vertical component, (d) Extracted radial component, (e) Extracted transverse component, (f) Extracted vertical component.

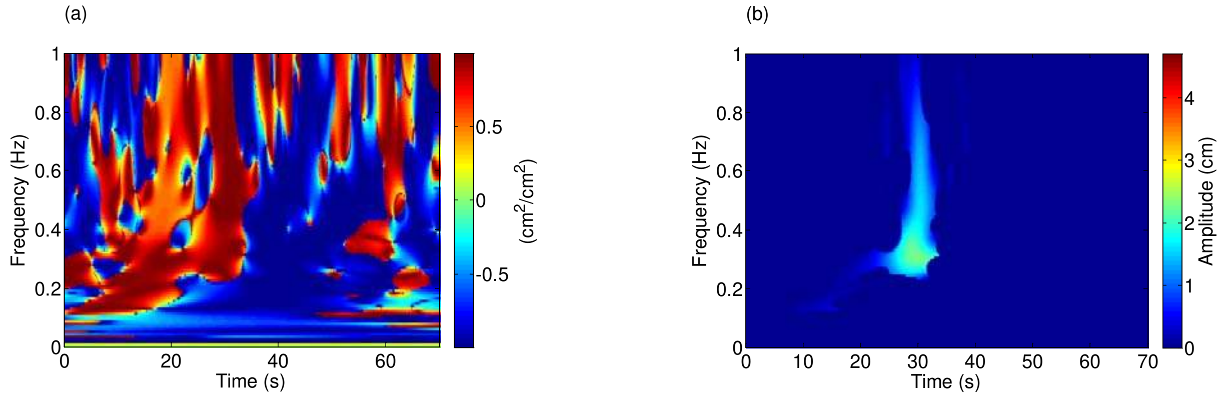

Figure 20. Extraction of pro-grade Rayleigh wave from recording at station TCU116. (a) Normalized inner product of and phase delayed component, (b) Amplitude of component filtered with the NIP criterion.

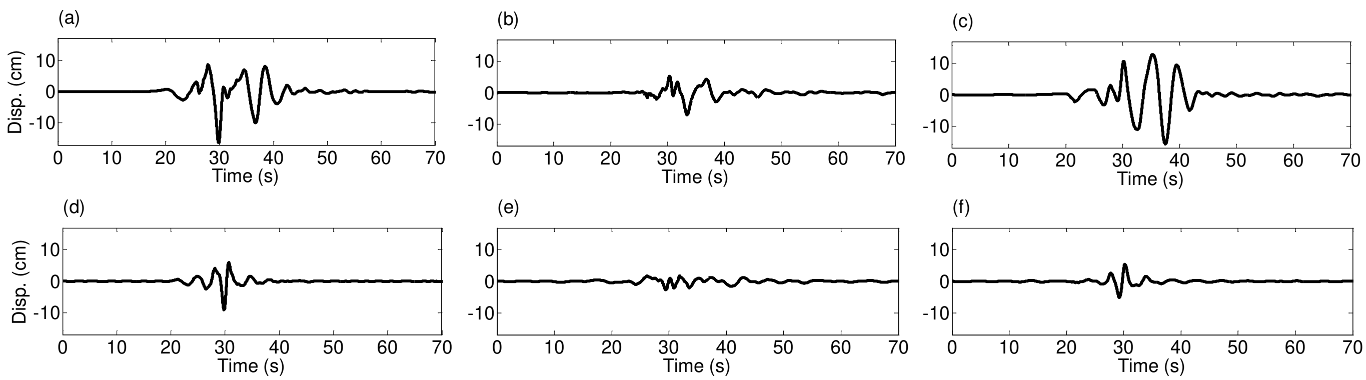

Figure 21. Rayleigh pro-grade wave extracted at station TCU116. (a) Unfiltered radial component, (b) Unfiltered transverse component, (c) Unfiltered vertical component, (d) Extracted radial component, (e) Extracted transverse component, (f) Extracted vertical component.

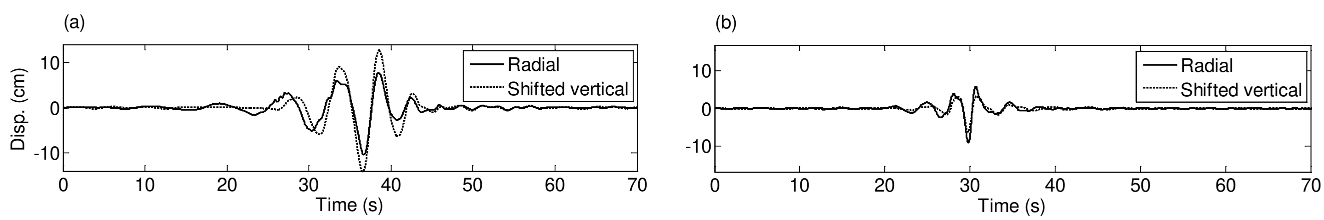

Figure 22. Comparison of radial and shifted vertical components of extracted Rayleigh waves at station TCU116. (a) Retro-grade wave, (b) Pro-grade wave.

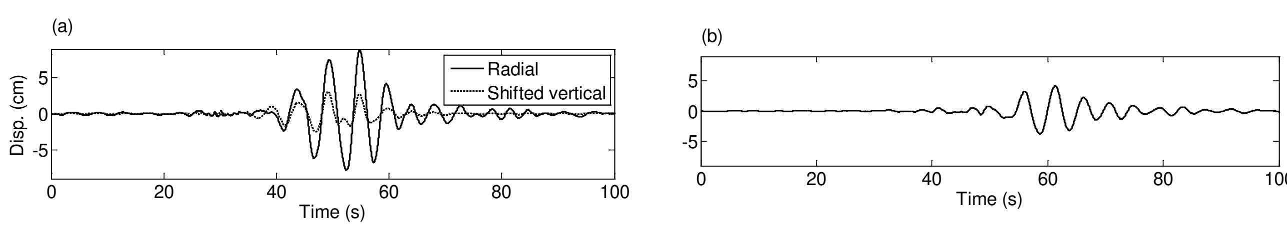

Figure 23. *R-T-V* displacement components of extracted waves at station TCU118. (a) Comparison of radial and shifted vertical component of retro-grade Rayleigh wave (b) Extracted (Love) wave in transverse direction.

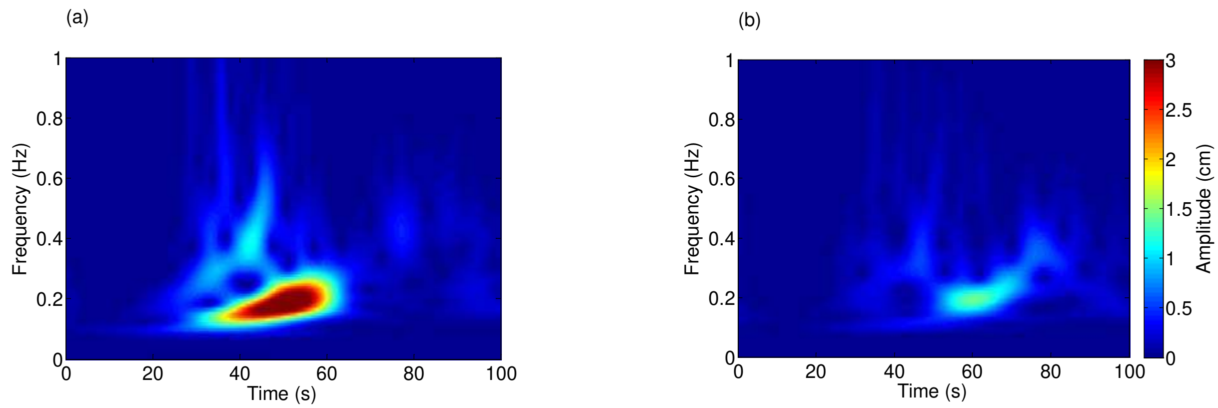

Figure 24. Radial and Transverse time-frequency components for unfiltered recording at station TCU118. (a) Amplitude of radial component (b) Amplitude of transverse component.

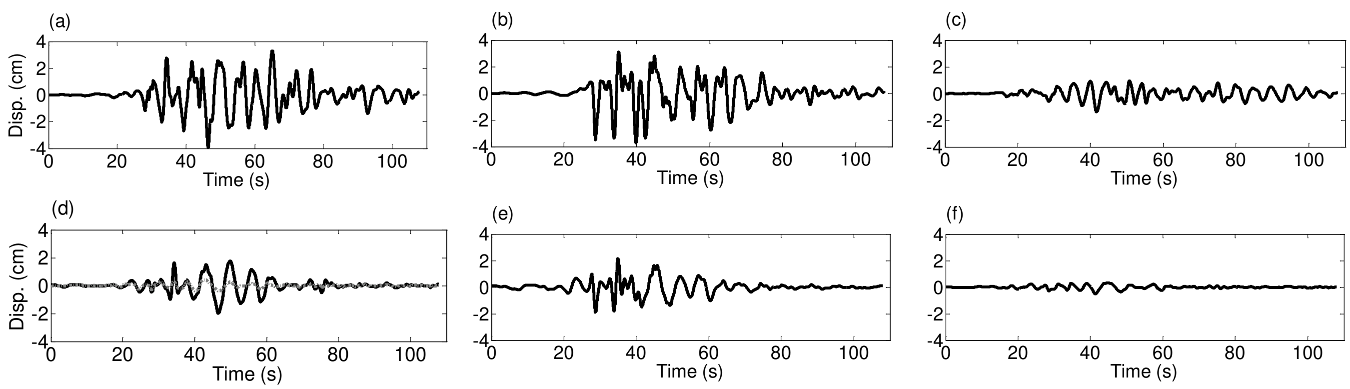

Figure 25. Extracted waves from recording at station CHY107. (a) Unfiltered radial component, (b) Unfiltered transverse component, (c) Unfiltered vertical component, (d) Extracted radial component (black line) and shifted vertical component (gray line), (e) Extracted transverse component, (f) Extracted vertical component.

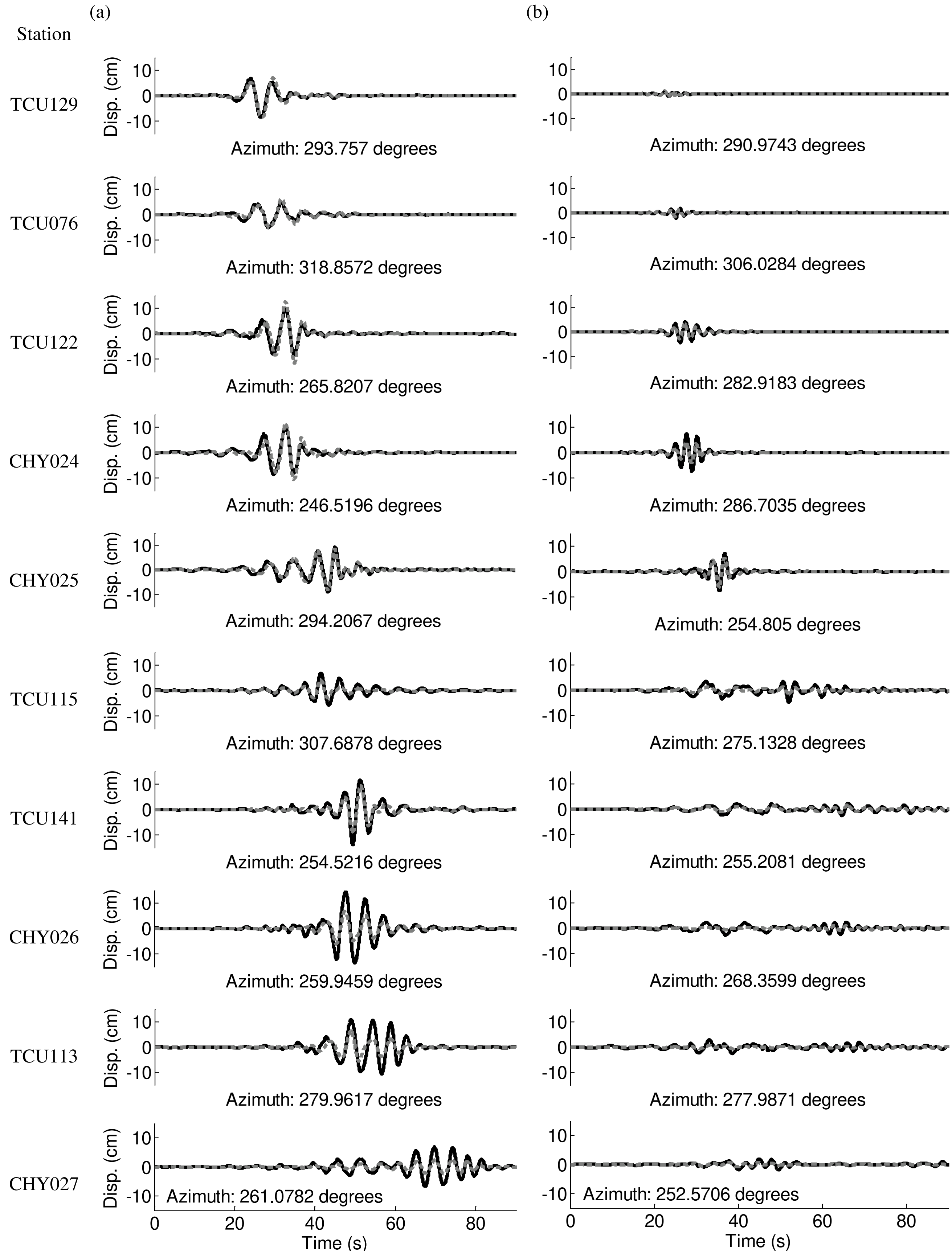

Figure 26. Radial component (black solid line) and shifted vertical component (gray dashed line) of extracted Rayleigh waves at different stations of the WCP plain in Taiwan. (a) Retro-grade waves, (b) Pro-grade waves.

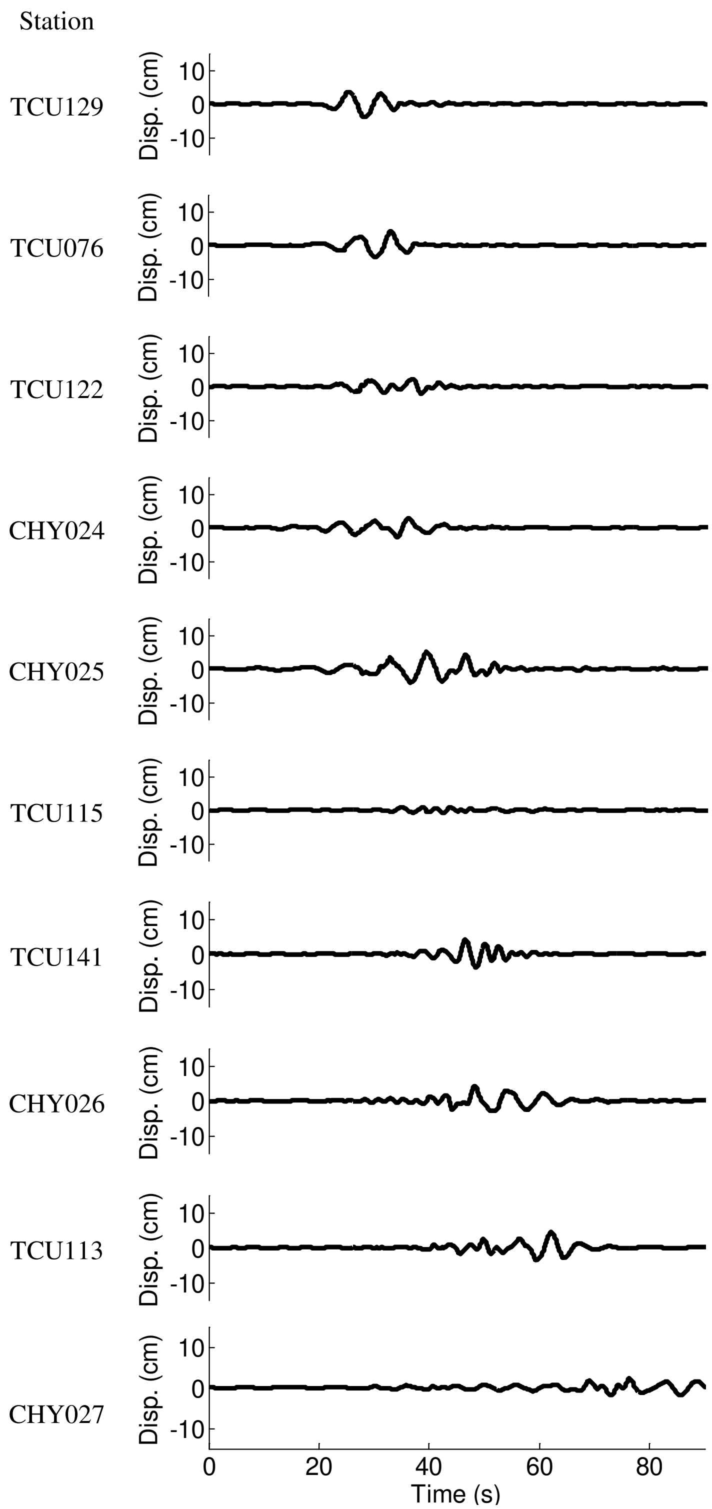

Figure 27. Extracted Love waves at different stations of the WCP plain in Taiwan.